CHEMISTRY OF MATERIALS
Article

Chem. Mater. **2010,** *22,* 3725–3734 3725
DOI:10.1021/cm100847p

Aluminosilicate Glasses As Yttrium Vectors for in situ Radiotherapy: Understanding Composition-Durability Effects through Molecular Dynamics Simulations

Jamieson K. Christie* and Antonio Tilocca

Department of Chemistry and Thomas Young Centre, University College London, London WC1H 0AJ, U.K.

Received March 24, 2010

The use of yttrium aluminosilicate (YAS) glasses as vectors for radiotherapy is critically affected by the glass durability in a physiological medium. To understand the relation between glass composition, structure, and durability at an atomistic level, we have carried out classical molecular dynamics (MD) simulations of two YAS compositions with different durability. The analysis of the MD trajectories shows that the lower durability at high Y_2O_3 concentration is due to the combined effect of lower connectivity of the glass network and reduced yttrium clustering. Increasing the yttrium content increased the coordination numbers of all atomic species, made possible a greater range of atomic environments, and reduced the network connectivity, particularly related to silicon. Aluminum ions show a strong tendency to self-aggregate, and can form additional Al−O−Al linkages to balance the reduced number of Si network-formers in the high Y_2O_3 composition: this leads to some very highly connected aluminum atoms, characterized by the appearance of large-*n* Q^n(Al) species in the corresponding distribution. The presence of significant yttrium clustering only in the more durable, low Y_2O_3 composition denotes that clustering of modifier ions can further enhance the glass durability, in agreement with previous results for bioactive glasses. (Tilocca et al. *Chem. Mater.* **2007**, *19*, 95.)

Introduction

Yttrium aluminosilicate (YAS) glasses are of interest both because of their technological importance and to improve our understanding of glass properties. In addition to their use as host materials in, for example, optics,[1] and additives to promote sintering of ceramics,[2] they also have application in the field of cancer radiotherapy.[3] Conventional radiotherapy irradiates tumors from a radiation source external to the body, which limits the largest dose that can be applied without damaging surrounding tissue. Internal, or in situ, radiotherapy relies instead on implanting a radioactive isotope into either the tumor or the arteries surrounding it, where the isotope can irradiate the tumor from within, substantially reducing damage to the surrounding healthy tissue.[3]

YAS glass microspheres containing 17.1 mol % Y_2O_3, 18.9 mol % Al_2O_3, and 64.0 mol % SiO_2 (YAS17) are used as the vector for the radioisotopes; the ^{90}Y isotopes, incorporated in the glass matrix, are excited to a radioactive state, and then injected into the blood vessels supporting the tumor, or into the tumor itself, where they remain during the treatment. This particular YAS17 composition was found empirically to have high chemical durability,[4] which is of critical importance for the safety of the patient: the glass should release as little yttrium as possible into the bloodstream while it is still radioactive (the half-life of ^{90}Y is 2.7 days). An understanding of how yttrium is incorporated into the glass network, and of other structural properties which can affect the solubility of the glass in a physiological medium, is clearly essential for further, rational progress in this field; however, the atomistic properties of YAS glasses are not well understood. Computer simulation allows us to examine the behavior of the glass at an atomistic level, and hence understand how specific properties depend on, for example, composition:[5] in this work we use classical molecular dynamics (MD) simulations to investigate the structure of YAS glass. Classical MD simulations allow us to study relatively large systems, with an overall accuracy determined by the interatomic potential employed.[6] Unbiased (parameter-free) simulations, such as Car−Parrinello molecular dynamics (CPMD),[7] are typically limited to a few hundreds of atoms. This limited size is suitable to investigate local properties such as the short-range and

*To whom correspondence should be addressed. E-mail: jamieson.christie@ucl.ac.uk

(1) Jander, P.; Brocklesby, W. S. *IEEE J. Quantum Electron.* **2004**, *40*, 509.
(2) Marchi, J.; Morais, D. S.; Schneider, J.; Bressiani, J. C.; Bressiani, A. H. A. *J. Non-Cryst. Solids* **2005**, *351*, 863–868.
(3) Chen, S.-D.; Hsueh, J.-F.; Tsai, S.-C.; Lin, W.-Y.; Cheng, K.-Y.; Wang, S.-J. *Nucl. Med. Commun.* **2001**, *22*, 121–125.
(4) Erbe, E. M.; Day, D. E. *J. Biomed. Mater. Res.* **1993**, *27*, 1301–1308.
(5) Tilocca, A.; Cormack, A. N.; de Leeuw, N. H. *Chem. Mater.* **2007**, *19*, 95–103.
(6) Frenkel, D.; Smit, B. *Understanding Molecular Simulations: From Algorithms to Applications*, 2nd ed.; Academic Press: New York, 1996.
(7) Car, R.; Parrinello, M. *Phys. Rev. Lett.* **1985**, *55*, 2471–2474.

Published on Web 05/20/2010

vibrational features,[8−12] but it would not allow us to investigate medium-range structural properties, such as the clustering behavior,[13,14] with adequate statistical detail.

There is a limited amount of previous data available on YAS glass, from computer simulation,[15] neutron and X-ray diffraction,[16] NMR[17,18] and IR spectroscopy;[2] even though none of these studies concern the compositions we are interested in, some general features are likely to be common. The picture which emerged is that of a disordered glass network containing mostly four-coordinated silicon and aluminum atoms, with yttrium acting as a network modifier having a higher coordination number and a larger bond distance to its neighboring oxygen atoms. It is difficult for standard experimental techniques to resolve the contributions from different atomic environments in amorphous structures, and computer simulations play an important role in this context.

In this paper, we describe the structure of two compositions of YAS glass with different amounts of yttrium. Short-range structural features such as partial pair-distribution functions and coordination numbers are calculated and found to agree with experimental and simulation data. The medium-range structure is of particular interest, and a thorough analysis is presented. This includes the wide range of oxygen environments found in the glass, the network connectivity and its decrease with increasing yttrium concentration, the nanoscale aggregation of yttrium and aluminum, and the preferential attachment of yttrium to aluminum over silicon. The decrease in network connectivity and reduced yttrium clustering in the models with a higher concentration of yttrium is linked to the experimentally observed lower durability.[4]

Simulation Details

Two compositions of YAS glass were studied: the first has 17.1 mol % Y_2O_3, 18.96 mol % Al_2O_3, and 63.94 mol % SiO_2, which is very close to the composition used in the radiotherapeutic applications mentioned,[3] and the second has 30 mol % Y_2O_3, 20 mol % Al_2O_3, and 50 mol % SiO_2. This second composition allows us to investigate the effect of increasing yttrium concentration on the glass properties. It has a chemical durability about one-third that of YAS17.[4] Throughout this work, these two compositions are referred to as YAS17 and YAS30, respectively.

Table 1. Buckingham Potential Parameters Used for the Simulation of YAS Glass

pairs	A (eV)	ρ (Å)	C (eV Å^6)
$O^{-1.2}$–$O^{-1.2}$	2029.2204	0.343645	192.28
$Si^{2.4}$–$O^{-1.2}$	13702.9050	0.193817	54.681
$Al^{1.8}$–$O^{-1.2}$	12201.417	0.195628	31.997
$Y^{1.8}$–$O^{-1.2}$	29526.977	0.211377	50.477

The classical interatomic potential model used is a pairwise Buckingham-type potential with the form

$$V_{ij}(r) = \frac{q_i q_j}{4\pi\varepsilon_0 r} + A_{ij}\exp(-r/\rho_{ij}) - C_{ij}/r^6 \qquad (1)$$

where V_{ij} is the potential energy between two atoms of species i and j at a separation r, q_i is the charge of atom i, and A_{ij}, ρ_{ij}, and C_{ij} are parameters of the model. The A, ρ, and C parameters used, reported in Table 1, have previously proven adequate to model the structure of amorphous oxides containing various amounts of yttrium, silicon, and aluminum.[15,19−21] We also verified the Y−O potential parameters by modeling a Y_2O_3 crystal with them, and showing that the optimized lattice constant was within 1% of the experimental value,[22] and the bulk modulus[23] within 10%.

Buckingham-type potentials have a well-known disadvantage: at small distances r, the power term dominates the exponential term, and a potential well is created, forcing pairs of atoms unphysically close. To avoid this problem, the Buckingham potential was replaced[20,24] at distances $r < r_c$, where r_c is the larger of the two values of r at which the energy is 70% of the maximum energy of the Buckingham potential, with a potential of the form B/r^n, where B and n are fitted to match smoothly the Buckingham potential and its first derivative at $r = r_c$.

Molecular dynamics simulations were carried out using the DL_POLY program[25] with a time step of 2 fs. Long-range Coulomb interactions were evaluated using the Ewald summation with a real-space sum cutoff of 12 Å, and short-range potentials were truncated at 8 Å.

The initial structures were generated by randomly placing about 2000 atoms with the correct composition into a cubic box such that the density was equal to the experimental density.[26] Four independent models at each composition were prepared. The YAS17 models had 92 Y_2O_3, 102 Al_2O_3, and 344 SiO_2 formula units and a box length of 29.9674 Å for a density of 3.2 g cm^{-3}, and the YAS30 models had 150 Y_2O_3, 100 Al_2O_3, and 250 SiO_2 formula units and a box length of 29.0591 Å for a density of 4.0 g cm^{-3}. To prevent atoms from starting unphysically close together, atoms were not initially placed closer than 80−90% of their typical interatomic distance. The melt-and-quench method was then used to prepare the models.[5] An NVT trajectory was

(8) Ispas, S.; Benoit, M.; Jund, P.; Jullien, R. *Phys. Rev. B* **2001**, *64*, 214206.
(9) Donadio, D.; Bernasconi, M.; Tassone, F. *Phys. Rev. B* **2004**, *70*, 214205.
(10) Massobrio, C.; Celino, M.; Pasquarello, A. *Phys. Rev. B* **2004**, *70*, 174202.
(11) Tilocca, A.; de Leeuw, N. H. *J. Phys. Chem. B* **2006**, *110*, 25810.
(12) Tilocca, A. *Phys. Rev. B* **2007**, *76*, 224202.
(13) Tilocca, A.; Cormack, A. N. *J. Phys. Chem. B* **2007**, *111*, 14256.
(14) Tilocca, A.; Cormack, A. N. *J. Phys. Chem. C* **2008**, *112*, 11936.
(15) Du, J. *J. Am. Ceram. Soc.* **2009**, *92*, 87–95.
(16) Pozdnyakova, I.; Sadiki, N.; Hennet, L.; Cristiglio, V.; Bytchkov, A.; Cuello, G. J.; Coutures, J. P.; Price, D. L. *J. Non-Cryst. Solids* **2008**, *354*, 2038–2044.
(17) Florian, P.; Sadiki, N.; Massiot, D.; Coutures, J. P. *J. Phys. Chem. B* **2007**, *111*, 9747–9757.
(18) Schaller, T.; Stebbins, J. F. *J. Phys. Chem. B* **1998**, *102*, 10690–10697.
(19) Du, J.; Cormack, A. N. *J. Non-Cryst. Solids* **2004**, *349*, 66–79. Erratum: Du, J.; Cormack, A. N. *J. Non-Cryst. Solids* **2005**, *351*, 956.
(20) Tilocca, A.; de Leeuw, N. H.; Cormack, A. N. *Phys. Rev. B* **2006**, *73*, 104209.
(21) Thomas, B. W. M.; Mead, R. N.; Mountjoy, G. *J. Phys.: Condens. Mat.* **2006**, *18*, 4697–4708.
(22) Ishibashi, H.; Shimomoto, K.; Nakahigashi, K. *J. Phys. Chem. Solids* **1994**, *5*, 809–814.
(23) Palko, J. W.; Kriven, W. M.; Sinogeikin, S. V.; Bass, J. D.; Sayir, A. *J. Appl. Phys.* **2001**, *89*, 7791.
(24) Bakaev, V. A.; Steele, W. A. *J. Chem. Phys.* **1999**, *111*, 9803.
(25) Smith, W.; Forester, T. R.; Todorov, I. T. DL_POLY is a molecular dynamics simulation package written by W. Smith, T. R. Forester, and I. T. Todorov and has been obtained from STFC's Daresbury Laboratory via the website http://www.ccp5.ac.uk/DL_POLY.
(26) Day, D. E.; Day, T. E. Radiotherapy glasses. In *An Introduction to Bioceramics*; Hench, L. L., Wilson, J., Eds.; World Scientific: River Edge, NJ, 1993; Chapter 17.

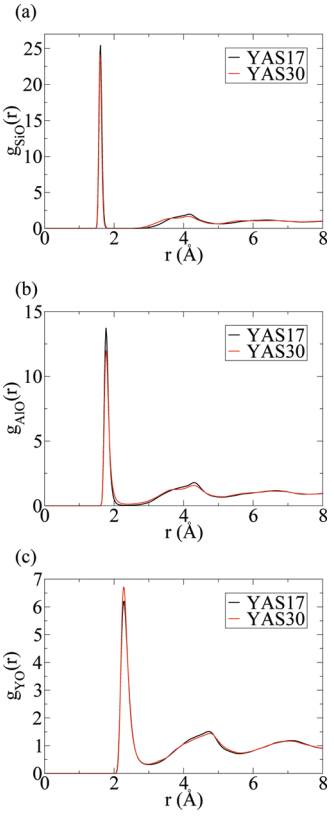

Figure 1. Partial pair-distribution functions (a) $g_{SiO}(r)$, (b) $g_{AlO}(r)$, and (c) $g_{YO}(r)$ for the YAS17 (black line) and YAS30 (red line) models.

run at 6000 K for 200 ps, to equilibrate the models above their melting temperature. The models were then continuously cooled to 300 K at a nominal cooling rate of 1 K/ps. Each model was then equilibrated at 300 K for 600 ps. The first 200 ps of these 300 K runs were discarded. The last 400 ps formed the production run, from which a total of 8000 configurations for each model were extracted, uniformly spaced every 50 fs. All data given in this paper are averaged over these 8000 configurations, and then over the four independent models.

Although the cooling rate of 1 K/ps is many orders of magnitude faster than cooling rates achieved experimentally, it is slower than the rate used in many other MD simulations of silicate glasses[12,15,20,27−33] which have given structural data in agreement with experimental results. We also simulated one model of each composition cooled at 10 K/ps, with all other parameters identical. We found that there was little difference between the structural properties of interest to us at the two cooling rates: a detailed comparison is reported in the Supporting Information section.

In addition, the convergence of the structural properties at 300 K was checked by dividing the 400 ps production run into four equal 100 ps blocks, and observing that the properties did not change between the four blocks.

(27) Cormack, A. N.; Du, J.; Zeitler, T. R. *Phys. Chem. Chem. Phys.* **2002**, *4*, 3193–3197.
(28) Pedone, A.; Malavasi, G.; Cormack, A. N.; Segre, U.; Menziani, M. C. *Theo. Chem. Acc.* **2008**, *120*, 557–564.
(29) Lusvardi, G.; Malavasi, G.; Tarsitano, F.; Menabure, L.; Menziani, M. C.; Pedone, A. *J. Phys. Chem. B* **2009**, *113*, 10331–10338.
(30) Linati, L.; Lusvardi, G.; Malavasi, G.; Menabure, L.; Menziani, M. C.; Mustarelli, P.; Pedone, A. *J. Non-Cryst. Solids* **2008**, *354*, 84–89.
(31) Liang, Y. F.; Miranda, C. R.; Scandolo, S. *Phys. Rev. B* **2007**, *75*, 024205.
(32) Du, J.; Benmore, C. J.; Corrales, R.; Hart, R. T.; Weber, J. K. R. *J. Phys.: Condens. Matter* **2009**, *21*, 205102.
(33) Mountjoy, G. *J. Non-Cryst. Solids* **2007**, *353*, 1849–1853.

Table 2. Amounts of Si, Al, and Y Atoms with Given Si−O, Al−O, and Y−O Coordination Numbers for the YAS17 and YAS30 Models[a]

	Si−O (%)		Al−O (%)		Y−O (%)	
coordination	YAS17	YAS30	YAS17	YAS30	YAS17	YAS30
3	0	0	0.719	0.012	5×10^{-4}	0
4	100.0	99.7	94.3	70.1	0.573	8×10^{-5}
5	6×10^{-5}	0.272	4.74	27.0	16.0	2.44
6	0	2×10^{-5}	0.240	2.87	54.4	35.7
7	0	0	0	0	25.8	47.4
8	0	0	0	0	3.16	13.6
9	0	0	0	0	0.176	0.866
10	0	0	0	0	0.003	0.004
average	4.00	4.00	4.05	4.33	6.16	6.75

[a] The cutoffs are taken from the first minimum in the partial $g(r)$'s (Figure 1).

Results

Short-Range Structure. *Silicon.* The mean Si−O distances of 1.614 Å in YAS17 and 1.607 Å in YAS30 (Figure 1a) are comparable to bond lengths of 1.60 Å found in MD and diffraction studies of YAS glass.[15,16] As in the diffraction study,[16] we find a slight decrease in the Si−O bond length with increasing yttrium content. The standard deviations of the distributions at 0.042 Å (YAS17) and 0.042 Å (YAS30) do not depend on composition. Almost all of the silicon atoms are four-coordinated (Table 2), with essentially no higher-coordinated silicon atoms in the YAS17 models, and 0.3% in the YAS30 models, again in agreement with previous experimental and modeling data,[15,16] which yielded coordination numbers of 3.9−4.0. The mean O−Si−O bond angles and their standard deviations (Figure 2a,b) are 109.4 ± 6.1 degrees (YAS17) and 109.3 ± 7.1 degrees (YAS30). As expected, because of the large amount of four-coordinated atoms, the peaks of these distributions are close to the ideal tetrahedral bond angle of 109.47 degrees. The slightly wider distribution in YAS30 is caused in part by the larger amount of five-coordinated silicon atoms.

Aluminum. The mean Al−O bond length is 1.806 Å in YAS17 and 1.832 Å in YAS30 (Figure 1b), which are comparable to values between 1.79 and 1.82 Å obtained in previous structural studies on YAS.[15,16] The slight reduction of the Al−O distance with decreasing yttria content is also seen in simulation,[15] although the reverse trend is found in experiment.[16] YAS30 has a slightly wider standard deviation of Al−O bond lengths of 0.118 Å, compared to 0.083 Å for YAS17.

NMR studies have consistently shown that aluminum coordination can range from four to six in YAS[17,18] and related[34] glasses, although four-coordinated is the most common. The exact populations are hard to quantify experimentally, although recent simulation models of low-silica YAS[15] showed that increasing the yttria content favors the formation of five- and six-coordinated aluminum atoms, such as those seen in Figure 3, a trend which we also find for the present compositions (Table 2).

(34) Sen, S.; Youngman, R. E. *J. Phys. Chem. B* **2004**, *108*, 7557–7564.

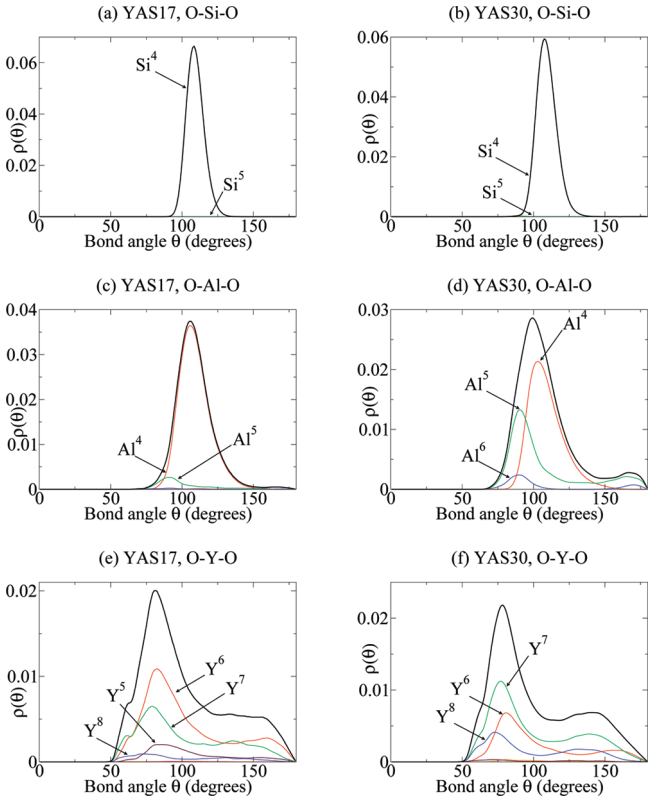

Figure 2. Bond-angle distributions for the O−Si−O angles for the (a) YAS17 and (b) YAS30 models, the O−Al−O angles for the (c) YAS17 and (d) YAS30 models, and the O−Y−O angles for the (e) YAS17 and (f) YAS30 models. The bold black line represents the total distribution, and the thinner colored lines represent the total from each coordination state of the cation, with the coordination number given in superscript.

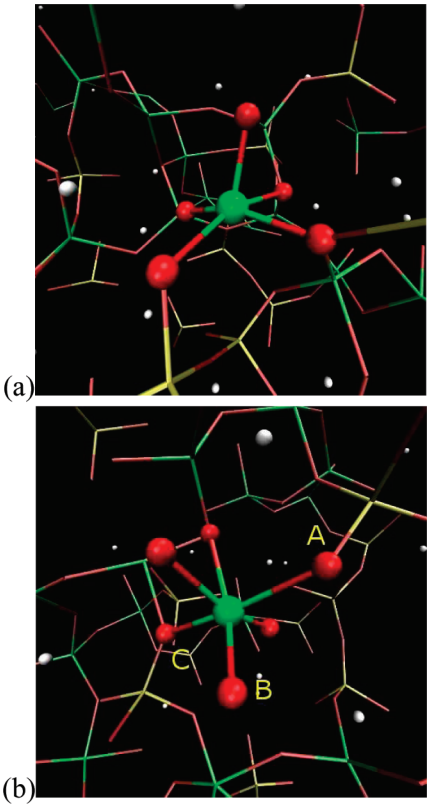

Figure 3. (a) A five-coordinated and (b) a six-coordinated aluminum atom. A, B, and C label oxygen atoms. Colors: aluminum (green), oxygen (red).

The coordination numbers of 4.05 (YAS17) and 4.33 (YAS30) are consistent with diffraction experiments, which gave 4.5 ± 0.5 for a glass with 11 mol % yttria.[16] The increased coordination number in YAS30 presumably explains its wider distribution of bond lengths.

This wider range of coordination environments is also visible in the O−Al−O bond-angle distributions (Figure 2c, d), which have means and standard deviations of 108.9 ± 13.0 degrees (YAS17) and 108.0 ± 20.4 degrees (YAS30). The YAS30 distribution is considerably wider because of the five- and six-coordinated aluminum atoms having peaks at angles close to 90 and 180 degrees, corresponding to angles from trigonal bipyramidal and octahedral coordination. Examples of these bond angles are shown in Figure 3b, in which bond angle O(A)−Al−O(B) is 88.3 degrees, and O(A)−Al−O(C) is 172.1 degrees.

Yttrium. The mean Y−O bond length is 2.399 Å in YAS17 and 2.391 Å in YAS30 (Figure 1c). Because of the asymmetric nature of the first peak in $g_{YO}(r)$, the peaks of the distributions are considerably lower at 2.28−2.29 Å for both models. This distance has not been measured experimentally for YAS glasses, but is close to distances of 2.32 Å[32] and 2.28 Å[35] for binary yttria-alumina glasses, as well as to the 2.31 Å Y−O distance in low-silica YAS models.[15]

The Y−O coordination number is 6.16 for YAS17 and 6.75 for YAS30 (Table 2), which compares well to experimental values of 6.9 ± 0.4[32] and 6.64 ± 0.33[35] for binary yttria-alumina glasses. Increasing the yttria content increases the coordination number, as found for low-silica YAS,[15] where the coordination numbers were in the range 6.5−7.3. A wider range of bonding environments is observed for yttrium than for either silicon or aluminum (Table 2): while six- and seven-coordinated yttrium atoms are most favorable, coordinations as low as three and as high as ten are observed (Table 2). As an example, a typical eight-coordinated yttrium atom is shown in Figure 4.

The O−Y−O bond-angle distribution (Figure 2e,f) shows a main peak at ∼80 degrees, and a secondary peak at ∼140 degrees. Because of the high coordination number, acute O−Y−O angles are to be expected as seen in Figure 4, where the O(A)−Y−O(B) bond angle is 57.7 degrees, and the O(C)−Y−O(D) bond angle is 74.4 degrees, and the main contribution to the first peak comes from six- and higher-coordinated yttrium atoms.

The role of yttrium in the network is rather different to that of silicon or aluminum. The different network behaviors of cations can be described using their field strength, defined as the cation's formal valence divided by the square of the sum of the oxygen radius and the cation radius while in 6-fold coordination.[18,36] Si^{4+} has a field

(35) Wilding, M. C.; Benmore, C. J.; McMillan, P. F. *J. Non-Cryst. Solids* **2002**, *297*, 143–155.

(36) *Fundamentals of Inorganic Glasses*; Varshneya, A. K., Ed.; Academic Press: New York, 1994.

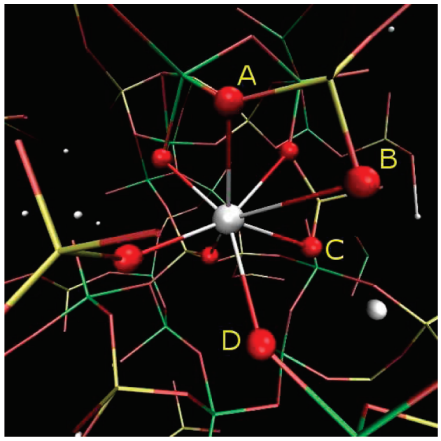

Figure 4. Eight-coordinated yttrium atom. A, B, C, and D label oxygen atoms. Colors: yttrium (white), oxygen (red).

strength of ~1.6, indicating a network former, and Al^{3+} has a field strength of ~0.9, indicating an intermediate behavior, closer to a network former.[36] Y^{3+} has a field strength of ~0.6,[18] indicating it is close to a network modifier, (cf. field strengths of the strong network modifiers Na (0.19) and Ca (0.33)).

The exact effects of yttrium on the glass structure are still poorly understood, in part because of various technical difficulties in carrying out ^{89}Y NMR (ref. 18 and references therein). Schaller and Stebbins[18] expect that yttrium (or other rare-earth analogues such as lanthanum) perturbs the glass network strongly, by stabilizing the formation of negatively charged species such as nonbridging oxygen atoms. We investigate this below.

Medium-Range Structure. In a pure silica glass, all oxygen atoms have the same environment — they are bonded to two silicon atoms (OSi_2) — and all silicon atoms are Q^4, meaning that they all have four bridging oxygen (BO) atoms as neighbors. Adding modifier atoms to silica glass will break Si−O−Si bonds, forming nonbridging oxygen (NBO) atoms, and modifying the oxygen environment and Q^n distributions considerably. In YAS glass, the glass network is formed from both silicon and aluminum cations interconnected via bridging oxygen atoms. Therefore, we define a bridging oxygen atom as any oxygen atom bonded to two or more silicon and aluminum cations (hence including atoms bonded to three network formers, known as TBO (three-bonded oxygen) atoms); all other oxygen atoms, including "free oxygen atoms", those not bonded to any network former, are non-bridging. Because these changes to the medium-range structural features strongly affect the durability of a glass in an aqueous medium,[14,37] it is important to study them in YAS glass, to understand how these features depend on the glass composition and yttrium content.

Oxygen Environments. The oxygen coordination numbers are shown in Table 3, and in Table 4 and Table 5 we present a detailed analysis of the oxygen coordination environments. From Table 3, we see that the O−Si coordination number is smaller and the O−Y larger in YAS30 than in YAS17, reflecting the smaller amount of silicon and larger amount of yttrium in YAS30. The

(37) Tilocca, A. *Proc. R. Soc. A* **2009**, *465*, 1003–1027.

Table 3. Average Coordination Numbers for the Oxygen Atoms

pair	YAS17	YAS30
O−Si	1.083	0.801
O−Al	0.650	0.692
O−Y	0.892	1.619
Total	2.625	3.112

Table 4. Oxygen Coordination Environments of the Non-Bridging Oxygen Atoms[a]

environment	YAS17 (%)	YAS30 (%)
OSi	1×10^{-5}	3×10^{-4}
$OSiY$	6.55	3.37
$OAlY$	0.382	0.178
OY_2	0.051	3×10^{-4}
$OSiY_2$	14.3	22.7
$OAlY_2$	4.33	6.73
OY_3	0.761	1.12
$OSiY_3$	1.26	6.36
$OAlY_3$	1.30	6.92
OY_4	0.410	2.57
$OSiY_4$	0.008	0.042
$OAlY_4$	0.025	0.415
OY_5	0	0.093
$OAlY_5$	0	0.001
OY_6	0	8×10^{-4}
total NBO	29.4	50.5

[a] Si, Al, and Y neighbors are included.

Table 5. Oxygen Coordination Environments of the Bridging Oxygen Atoms[a]

environment	YAS17 (%)	YAS30 (%)
$OSiAl$	15.2	4.94
OSi_2	19.6	5.18
OAl_2	1.10	0.355
$OSiAl_2$	2.19	1.80
OSi_2Al	0.476	0.039
$OSiAlY$	18.1	18.0
OAl_2Y	5.86	6.13
OSi_2Y	4.75	4.14
OAl_3	1.03	0.78
$OSiAlY_2$	0.895	3.38
OSi_2Y_2	0.047	0.203
OAl_2Y_2	1.16	3.52
$OSiAl_2Y$	0.071	0.320
OSi_2AlY	0	0.003
$OSiAl_3$	0	0.001
OAl_3Y	0.100	0.573
OAl_4	0	0.014
OAl_2Y_3	0.011	0.086
OAl_3Y_2	0.026	0.016
OAl_4Y	0	1×10^{-5}
OSi_2Y_3	2×10^{-6}	1×10^{-5}
$OSiAl_3Y$	0	5×10^{-6}
$OSiAlY_3$	2×10^{-5}	0.045
$OSiAl_2Y_2$	0	3×10^{-4}
OAl_2Y_4	0	1×10^{-4}
OAl_3Y_3	0	8×10^{-4}
total BO	70.6	49.5

[a] Si, Al, and Y neighbors are included.

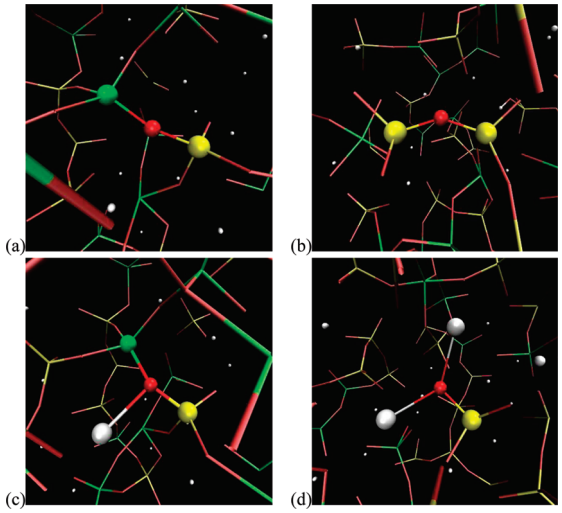

Figure 5. Oxygen atoms in the (a) OSiAl, (b) OSi_2, (c) OSiAlY, and (d) $OSiY_2$ environments. Colors: oxygen (red), silicon (yellow), aluminum (green), yttrium (white).

O−Al coordination number is slightly larger in YAS30, presumably because of the larger Al−O coordination number.

From Table 4 and Table 5, we see that most oxygen atoms in YAS17 have two or three neighbors (Si, Al, and Y species), and most oxygen atoms in YAS30 have three or four: the average O coordination number rises from 2.62 to 3.11. A similar increase is seen in MD simulations of binary yttria-alumina glasses with increasing yttrium content.[32] Yttrium modifies the network and creates more non-bridging oxygen atoms: the amount of NBOs rises from 29% (YAS17) to 51% (YAS30) as the yttrium concentration is increased.

In the YAS17 models, the four most common oxygen environments are (a) OSiAl, (b) OSi_2, (c) OSiAlY, and (d) $OSiY_2$, together making up about two-thirds of the oxygen coordination states (Figure 5). Environments (a) and (b) are bridging oxygen atoms in a regular glass network, while (c), a bridging oxygen, and (d), a non-bridging oxygen, also involve coordination to network-modifying yttrium atoms. The YAS30 models show a wider range of oxygen environments: the two dominant configurations are (c) and (d) above, and the percentage of oxygen atoms in configuration (d) is larger in YAS30 than in YAS17. In addition, several environments found in YAS30, particularly those with high coordination numbers, are only minimally populated (if at all) in the YAS17 models.

It is clear also from Table 3 that there is substantial coordination of oxygen to modifier ions, as observed in calcium/sodium silicate glasses.[33] Previous MD studies[11,33] also suggest that non-bridging oxygen atoms bond more strongly to modifiers than bridging oxygens do. This is confirmed for YAS glass by computing (Table 4 and Table 5) that the NBO-Y coordination number is higher than the BO-Y coordination number: in YAS17 it is 0.56 compared to 0.33, and in YAS30 it is 1.18 compared to 0.44. The rule of thumb that oxygen atoms are not more than four-coordinated[33] is broadly obeyed as well, with 0.07% (YAS17) and 0.7% (YAS30) of oxygen atoms so bonded. The number of TBOs decreases slightly from 3.9% in YAS17 to 3.5% in YAS30.

A previous ^{17}O NMR study[18] was able to assign three peaks: one peak from oxygen atoms bonded to two tetrahedral (T) cations, one peak from oxygen atoms bonded to a single T and one or more yttrium atoms, and one peak which was tentatively assigned to oxygen atoms bonded to a single T and more yttrium neighbors than the previous peak. All these environments are seen in our simulations (Table 4 and Table 5).

Our simulations show that 1.2% of oxygen atoms in YAS17 and 3.8% in YAS30 are so-called "free" oxygen ions, that is, they are not bound into the glass network of Si and Al, and coordinate only network-modifying yttrium atoms. While the same NMR study[18] was unable to identify any such oxygen atoms, they were observed experimentally[38] in other rare-earth glasses: lanthanum-containing silicate and alkali silicate glass, and in simulation[39] of lanthanum-containing silicate and soda silicate glass. It is probable that the small quantities of free oxygen ions in YAS glass were below the sensitivity of the experiment. The expected relatively high mobility of these non-bonded oxygen atoms could play an important role in the lower durability of YAS30.

On the basis of bond-valence considerations,[17,18] the oxygen atom in an Si−O−Al link should not be bonded to more than one yttrium atom, and oxygen atoms in the OAl_3 environment should be more common than those in the OSi_3 environment. However, at variance with these predictions, our simulations show that small percentages (2.6% in YAS17 and 13.0% in YAS30) of Si−O−Al oxygen atoms are actually coordinated to two or more yttrium atoms.

As expected, there is no oxygen atom with more than two silicon neighbors, while about 1.2% (YAS17) and 1.4% (YAS30) of oxygen atoms have more than two aluminum neighbors. It is clear that high-coordinated oxygen atoms bond preferentially to aluminum rather than silicon. Some of these atoms (1.0% in YAS17 and 0.8% in YAS30) form OAl_3 oxygen triclusters. This has been proposed as a charge-balancing configuration, and has been observed in NMR studies of aluminosilicate glasses,[40] as well as in MD simulation of low-silica YAS glass.[15] As discussed below, formation of OAl_3 species appears to promote aggregation of Al ions in these glasses.

Q^n distributions. The medium-range structure of the network can be further defined by studying the Q^n distributions. Because the Q^n distribution and the number of Si−O−Al bonds affect the ^{29}Si NMR chemical shift,[2] NMR data can provide important insight on this property; MD simulations are extremely useful to interpret the NMR data, given that the Q^n distribution of a glass composition can be *directly* extracted from a suitable

(38) Wilding, M. C.; Navrotsky, A. *J. Non-Cryst. Solids* **2000**, *265*, 238–251.
(39) Corrales, L. R. *J. Non-Cryst. Solids* **2005**, *351*, 401–408.
(40) Schmücker, M.; Schneider, H. *J. Non-Cryst. Solids* **2002**, *311*, 211–215.

Table 6. Total Q^n Distributions and Network Connectivities (NC) for the Si and Al Cations in the YAS17 and YAS30 Models

	Si (%)		Al (%)	
n	YAS17	YAS30	YAS17	YAS30
0	0.19	2.64	0	0.250
1	3.17	16.5	0.517	2.83
2	16.1	34.2	3.73	12.9
3	39.2	33.5	27.3	36.1
4	41.4	13.1	65.4	34.0
5	4×10^{-5}	2×10^{-5}	2.85	12.8
6	0	0	0.203	1.16
NC	3.184	2.381	3.670	3.437

trajectory. The YAS glass network involves only silicon and aluminum atoms, since yttrium is not a network former. We define the partial and total Q^n distributions of network-forming species A and B as follows. The *total* Q^n for a specific atom x of species A is the number n of bridging oxygen atoms bound to x, where a bridging oxygen is an oxygen bound to x and at least one more A or B; the corresponding network connectivity (NC) of species A is calculated as the weighted average of the total Q^n(A), and represents the *average* number of BO in the coordination shell of A.[13] The network connectivity is an effective descriptor of the durability of a glass in an aqueous physiological medium: a low (~2) silicon network connectivity characterizes more soluble and thus highly bioactive glass compositions, whereas nonbioactive compositions have an NC greater than 3.[37]

The *partial* A−B Q^n is defined as the number n of A−O−B linkages which start from the same atom x of type A and lead to an atom of type B. Each A−O−B linkage is counted, even if two or more share the same central oxygen atom. Because of the presence of three- and higher-coordinated oxygen atoms (Table 4 and Table 5), this definition of partial Q^n implies that the average n calculated from the partial Q^n can exceed the A−O coordination number, and that the sum of the partial Q^n is not equal to the total Q^n.

The total Q^n distributions and network connectivities are given in Table 6 and the partial Q^n distributions are given in Table 7. Our models show the co-existence of several different Q^n species (Table 6 and Table 7), in contrast to the predictions of binary and ternary models which allow for only two or three.[41] Raman and NMR spectra of modified silicate glasses had suggested the coexistence of at least three different Q^n species for silicon in these materials.[42,43]

The total Q^n distribution and the network connectivity (Table 6) reveal that silicon is substantially less interconnected in YAS30 than in YAS17. A net reduction in connectivity is to be expected, since the increased amount of yttrium modifies the network which would lead to lower connectivity overall. But the reduction in the total

Table 7. Partial Q^n Distributions and Partial Connectivities (PC) for the Si and Al Cations in the YAS17 and YAS30 Models

	Si−Si (%)		Si−Al (%)		Al−Si (%)		Al−Al (%)	
n	YAS17	YAS30	YAS17	YAS30	YAS17	YAS30	YAS17	YAS30
0	9.16	33.4	17.9	17.9	2.49	9.02	15.6	13.0
1	30.2	43.2	37.9	35.4	13.1	29.0	31.0	24.3
2	34.2	18.6	27.5	27.7	35.5	32.1	29.3	28.6
3	20.7	4.16	13.4	14.0	33.8	22.6	16.5	20.3
4	5.74	0.700	2.78	4.16	14.0	5.81	5.15	9.03
5	0	0	0.161	0.435	0.955	1.17	1.81	2.91
6	0	0	0.073	0.012	0.113	0.287	0.593	1.117
7	0	0	0	3×10^{-4}	0.008	0.004	0.002	0.469
8	0	0	0	0	0	0	0	0.095
9	0	0	0	0	0	0	0	0.097
PC	1.837	0.956	1.466	1.535	2.472	1.918	1.725	2.050

aluminum connectivity is rather smaller, implying that it is much less affected by the network modification than silicon: Al compensates the loss of Si neighbors in YAS30 by forming additional Al−O−Al linkages (Table 7). As the yttrium concentration increases, both the Si−Si and Al−Si partial Q^n connectivity decrease (Table 7) because there are fewer silicon atoms to which to connect. The Si−Al average partial connectivity barely changes because the amount of aluminum is close to constant. However, the Al−Al average partial connectivity increases substantially, indicating that the aluminum atoms, although unchanged in number, are more closely connected in YAS30. In particular, the long tail of the Al−Al partial Q^n distribution with n as high as nine is caused by one or more aluminum atoms bonded to three- and four-coordinated oxygen atoms. It is clear that the presence of yttrium, which increases the coordination number of all the cations as well as oxygen, and the preferential attachment of high-coordinated oxygen to aluminum, leads to a much more closely interconnected Al network at higher yttrium content.

Intertetrahedral Bond-Angle Distributions. Figure 6 and Figure 7 show the bond-angle distributions centered on the oxygen atoms. The Si−O−Si bond-angle distributions (Figure 6a and Figure 7a) are peaked at about 150 degrees (YAS17) and 135 degrees (YAS30), with a broad range of angles. This shift in peak is caused by the reduction in the amount of OSi_2 oxygen atoms in YAS30. The decomposition into the individual angle contributions, highlighted in the figures, shows that wider angles are typically those of a central oxygen bonded to two silicon atoms, while angles centered on higher-coordinated oxygen are lower, because of the steric hindrance of the third neighbor.[5]

The Si−O−Al bond-angle distribution (Figure 6b and Figure 7b) shows much the same features, with low-coordinated oxygen atoms having higher bond angles than high-coordinated oxygen atoms. The Al−O−Al bond-angle distributions (Figure 6c and Figure 7c) show more peaks in the overall distribution, also with lower-coordinated aluminum atoms having higher bond angles than higher-coordinated aluminum atoms.

In the Y−O−Y bond-angle distributions (Figure 6d and Figure 7d), it seems that the bond angle is not particularly dependent on the oxygen environment, since

(41) Dupree, R.; Holland, D.; Mortuza, M. G. *J. Non-Cryst. Solids* **1990**, *116*, 148–160.
(42) Lin, C.-C.; Huang, L.-C.; Shen, P. *J. Non-Cryst. Solids* **2005**, *351*, 3195–3203.
(43) Maekawa, H.; Maekawa, T.; Kawamura, K.; Yokokawa, T. *J. Non-Cryst. Solids* **1991**, *127*, 53–64.

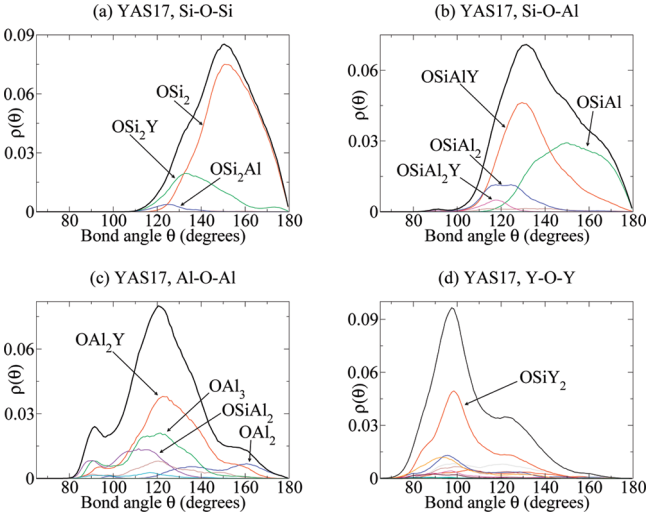

Figure 6. (a) Si−O−Si, (b) Si−O−Al, (c) Al−O−Al, and (d) Y−O−Y bond-angle distributions for the YAS17 models. The bold line represents the total distribution, and the regular lines represent the total from each oxygen coordination state, labeled with the bonded atoms.

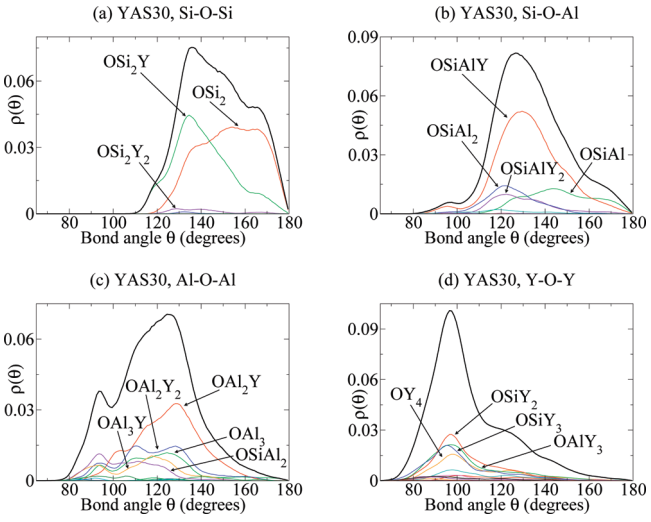

Figure 7. (a) Si−O−Si, (b) Si−O−Al, (c) Al−O−Al, and (d) Y−O−Y bond-angle distributions for the YAS30 models. The bold line represents the total distribution, and the regular lines represent the total from each oxygen coordination state, labeled with the bonded atoms.

the distribution is composed of several contributions, all of which roughly reflect the shape of the total distribution, which peaks just below 100 degrees, regardless of composition.

Inhomogeneities and Preferential Attachment. The distribution of the cations on the medium-range length scale is also important for the glass durability in solution. Clustering and aggregation on these length scales has been suggested[37,44] as an inhibitor of bioactivity in bioactive glasses, and it is known that clustering of modifiers can affect ionic transport.[45]

In low-silica YAS glasses, sharper peaks in $g_{YY}(r)$ and $g_{YAl}(r)$ than in $g_{YSi}(r)$ were attributed to yttrium forming clusters with itself and with aluminum, but not with silicon.[15]

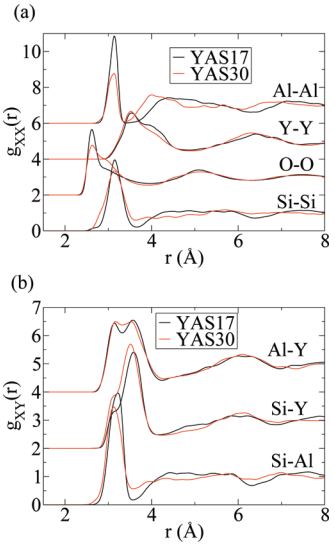

Figure 8. Partial pair-correlation functions for (a) $g_{OO}(r)$, $g_{SiSi}(r)$, $g_{AlAl}(r)$, $g_{YY}(r)$ and (b) $g_{SiAl}(r)$, $g_{SiY}(r)$, $g_{AlY}(r)$ for the YAS17 and YAS30 models. Some functions are vertically offset for clarity.

Cation−cation and self−self partial pair-distribution functions for our models are given in Figure 8. If, as in the present case, one wants to compare the tendency to form clusters in two compositions containing different amounts of Si and Y ions, direct comparison of the raw $g(r)$'s can hardly expose the relevant differences. Instead, we compute the observed coordination number N_{obs}, which is the integral of $g(r)$ up to its first minimum, and compare it to that expected if the same density of ions were positioned randomly and uniformly throughout the glass. If atoms of one species were homogeneously distributed throughout the model, and the nearest-neighbor distance cutoff were r_c, then the homogeneous coordination number N_{hom} would be $(4/3)\pi r_c^3\rho - 1$, where ρ is the number density of the specific type of atoms.[5] N_{obs} can be compared to this value, and the ratio $r = N_{obs}/N_{hom}$ of these quantities can be adopted as a measure of clustering, with deviations from unity denoting clustering.[13,46]

In principle, this analysis could be carried out with respect to any distance, but we use the cutoff r_c corresponding to the first coordination shell, as that is where the nanoscale aggregation we are interested in will be apparent. Moreover, using the second coordination shell would not be straightforward, because for some atom pairs in these models, this shell is not as well-defined as the first (Figure 8).

The $r = N_{obs}/N_{hom}$ clustering factors are reported in Table 8. The observed raw Y−Y coordination numbers are 3.14 in YAS17 and 5.44 in YAS30, corresponding to clustering ratios r_{Y-Y} of 1.47 for YAS17 and 1.11 for YAS30, denoting that yttrium clustering is only substantial at lower yttrium concentration. Similar results were found for modified soda-lime silicate glasses, for which calcium nanoaggregates are mostly formed at higher silicon concentration.[5,44] Table 8 also denotes aggregation of Y to

(44) Tilocca, A.; Cormack, A. N. *Nuovo Cimento B* **2008**, *123*, 1415.
(45) Lammert, H.; Heuer, A. *Phys. Rev. B* **2005**, *72*, 214202.
(46) Mead, R. N.; Mountjoy, G. *J. Phys. Chem. B* **2006**, *110*, 14273–78.

Table 8. Clustering Ratios $r = N_{obs}/N_{hom}$ for Pairs of Cations in the Two Models[a]

pair	YAS17	YAS30
Y−Y	1.47 ± 0.10	1.11 ± 0.05
Y−Si	1.42 ± 0.07	1.64 ± 0.10
Y−Al	1.89 ± 0.02	1.65 ± 0.14
Si−Si	1.18 ± 0.08	1.02 ± 0.09
Si−Al	3.25 ± 0.18	2.67 ± 0.27
Al−Al	5.44 ± 0.53	4.85 ± 0.26

[a] Larger ratios imply more clustering. The error bars are the standard deviations of the clustering ratios of the four independent models.

both Si and Al, with the highest aggregation shown by Y−Al in YAS17. No significant Si−Si aggregation is observed, whereas Al strongly aggregates with other Al and with Si. To summarize this analysis, the low-yttria composition is characterized by more marked clustering behavior (mostly involving Y and Al ions) compared to YAS30.

Schaller and Stebbins[18] state that is difficult to deduce whether yttrium bonds preferentially to silicon or aluminum because of the lack of NMR data on model compounds. The analysis of Table 8 has highlighted preferential Y−Al than Y−Si aggregation, but only in YAS17. This effect can be further examined by counting the number of Y−O−Si and Y−O−Al links and normalizing by the number of silicon or aluminum atoms, respectively. This is equivalent to computing the Y−Si and Y−Al partial Q^n distributions, if the definition of Q^n is stretched to include a network-modifying cation. YAS17 has 2.533 Y−O−Si links per Si atom and 3.111 Y−O−Al links per Al atom, compared to YAS30, which has 5.113 Y−O−Si links per Si atom and 5.644 Y−O−Al links per Al atom. We thus find that yttrium prefers to bind to aluminum, and this preference is stronger at low yttrium concentrations.

This strong aggregation of aluminum reflects several factors. The Al−O−Al bond angle (Figure 6c and Figure 7c) peaks at a much smaller angle, ∼120−125 degrees, than the Si−O−Si bond angle (Figure 6a and Figure 7a), which peaks at ∼135−150 degrees. This gives a smaller Al−Al first-neighbor distance (Figure 8a), showing that Al ions can be packed more tightly around a single oxygen atom than the higher-charge Si ions. The fact that OAl_3 triclusters exist in the models, but OSi_3 do not, denotes that these species are linked to, and possibly involved in, Al aggregation. Also, we see from Table 7 that Al−O−Al bonds are preferred to Al−O−Si: YAS17 has 1.725 Al−O−Al bonds per Al atom, compared to 1.466 Al−O−Si per Si, while YAS30 has 2.05 Al−O−Al bonds per Al atom, compared to 1.535 Al−O−Si per Si. These effects are clearly related to each other, and their combination is responsible for the strong self-aggregation of Al, further illustrated in Figure 9. The figure highlights two regions of YAS30 in which aluminum has aggregated, along with structural features that the previous analysis has linked to this aggregation, that is, high-coordinated aluminum and oxygen atoms, and $Al(O_2)Al$ two-membered rings.

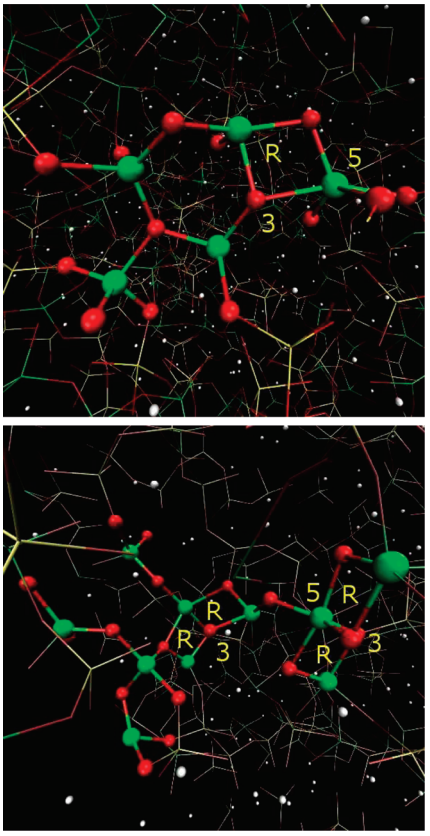

Figure 9. Two snapshots from YAS30 models, highlighting aluminum aggregation, and three-coordinated oxygen atoms (labeled "3"), five-coordinated aluminum atoms (labeled "5"), and $Al(O_2)Al$ two-membered rings (labeled "R"). Colors: aluminum (green), oxygen (red).

Structural links between oxygen triclusters and $Al(O_2)Al$ two-membered rings have previously been observed in aluminosilicate glass.[47,48]

Final Remarks

Our simulations have shown that the structure of YAS glass is that of a disordered glass network containing silicon and aluminum as network-forming cations and yttrium as a network-modifying cation. While silicon is almost entirely four-coordinated, aluminum ranges from four- to six-coordinated, and yttrium can have a wider range of coordination numbers, with six and seven being most common. The good agreement of the short-range structure (coordination numbers and bond lengths) with experimental data confirms the accuracy of the model, and allows us to focus on the medium-range features extracted from the MD trajectories.

Increasing the yttrium content increases all cation-oxygen coordination numbers, and gives a greater range of oxygen environments. Most oxygen atoms have two, three, or four neighbors, depending on composition, and the concentration of non-bridging oxygen atoms increases with increasing yttrium concentration, as expected. By directly examining the atomic trajectories, we are able to observe oxygen environments which have previously been

(47) Pfleiderer, P.; Horbach, J.; Binder, K. *Chem. Geol.* **2006**, *229*, 186–197.

(48) Winkler, A.; Horbach, J.; Kob, W.; Binder, K. *J. Chem. Phys.* **2004**, *120*, 384–393.

speculated to exist:[18] specifically, we find a small amount of oxygen atoms forming OAl_3 triclusters, and some nonbonded, isolated oxygen atoms which are only coordinated to yttrium.

The Q^n distributions reveal that Si and Al species with several different values of n coexist in the glass. Increasing the yttrium content substantially reduces the silicon connectivity, but only slightly affects the aluminum connectivity: aluminum compensates for the lack of silicon neighbors at higher yttrium concentration by forming additional Al−O−Al linkages. The reduction in silicon network connectivity with increasing yttrium implies a more fragmented glass network, which reduces durability of the glass. For the high-yttrium composition, the increased Al−O coordination and the observed preference of high-coordinated oxygen atoms to bond to aluminum favor the formation of Al nanoaggregates: these regions are characterized by some Q^n(Al) species with unusually high (up to 8−9) values of n: structural features such as $Al(O_2)Al$ rings and oxygen triclusters (Figure 9) appear to be associated with enhanced Al aggregation.

Whereas both compositions are characterized by aggregation of Al network-formers, the more durable YAS17 glass also shows clustering of network-modifier yttrium ions: in line with recent suggestions that clustering of modifier cations inhibits the bioactivity of bioglasses by reducing their dissolution rate,[5,13,14] the present results show that yttrium clustering enhances the durability of YAS glass, probably by hindering the migration process of these cations in the bulk. However, even though some of the structural effects highlighted here affect ion migration, our simulations did not directly address the diffusion of yttrium through the glass network: this is an obvious route for further work.

The present results allow us to understand the structural changes that Si→Y substitution determine in YAS compositions, and rationalize these changes with respect to the applications of these glasses in radiotherapy. Increasing the yttrium concentration reduces the silicate network connectivity, and reduces the clustering of the modifying yttrium atoms; both effects will promote faster dissolution of the glass, thus explaining the experimentally observed increase in solubility in YAS30 compared to YAS17.[4] Going from YAS17 to the less durable YAS30, the silica network connectivity decreases from a value above 3, typical of low-solubility bioinactive glass compositions, to a value approaching 2, characteristic of highly soluble bioactive phases.[37] Moreover, the simulations denote that the silica, rather than alumina, fraction determines the yttrium release rate of these materials because of the ability of Al to keep its network connectivity unchanged by forming Al−O−Al links to replace Al−O−Si lost upon Si→Y substitution.

Finally, this work shows the potential of MD simulations to support the rational optimization of glass properties. For instance, once the relationship between the above structural features and the glass composition is established, the glass solubility could be tailored toward the best values required for specific radiotherapy applications.

Acknowledgment. The EPSRC (Grant no. EP/F020066/1) and the U.K.'s Royal Society (University Research Fellowship for A.T.) are gratefully acknowledged for financial support. The authors also acknowledge the use of the UCL Legion High Performance Computing Facility, and associated support services, in the completion of this work.

Supporting Information Available: Additional information on the simulation details and results as noted in the text. This material is available free of charge via the Internet at http://pubs.acs.org.